

Field-Effect Transistors Based on Single Nanowires of Conducting Polymers

Adam K. Wanekaya,^{†,§} Mangesh A. Bangar,[†] Minhee Yun,[‡] Wilfred Chen,[†]
Nosang V. Myung,^{*,†} and Ashok Mulchandani^{*,†}

Department of Chemical and Environmental Engineering and Center for Nanoscale Science and Engineering, University of California, Riverside, California 92521, and Department of Electrical and Computer Engineering, University of Pittsburgh, Pittsburgh, Pennsylvania 15261

Received: November 1, 2006; In Final Form: January 30, 2007

Field-effect transistors based on single nanowires of conducting polymers (i.e., polyaniline and polypyrrole) were fabricated and characterized. The 100-nm-wide and 2.5- μm -long conducting polymer nanowire field-effect transistors were turned “on” and “off” by electrical or chemical signals. A large modulation in the electrical conductivity of up to 3 orders of magnitude was demonstrated as a result of varying the electrochemical gate potential of these nanowires. Single nanowire conducting polymer field-effect transistors show higher electrical performance than field-effect transistors based on conducting polymer nanowire electrode junctions and thin films in terms of their transconductance (g_m) and on/off current ($I_{\text{on}}/I_{\text{off}}$) ratio. Furthermore, the performance of single nanowires conducting polymer field-effect transistors was found to be comparable to the silicon nanowire field-effect transistors. These results imply that it is possible to tune the sensitivities of these conducting polymer nanowires by simple control of the electrolyte/liquid ion gate potentials. On the basis of these findings, we demonstrated the ability to tailor the sensitivities of sensors based on single conducting polymer nanowires.

Introduction

Organic conducting polymers have found application in electronics as field-effect transistors and sensors because of their unique properties. For example, the electrical conductivity of these polymers can vary from an insulator to almost the metallic state and be reversibly modulated over 15-orders of magnitude by controlling the dopant type and level. More recently, several research groups, including ours, have synthesized nanowires of organic conducting polymers (CPNWs) such as polyaniline, polypyrrole, poly(3,4-ethylenedioxythiophene), etc. at ambient conditions through well-known chemical and electrochemical procedures.^{1,2} Unlike inorganic one-dimensional (1-D) nanostructured materials that usually require high operating temperatures in ultrahigh vacuum, CPNWs can be synthesized under ambient conditions in a cost-effective manner.

One promising application of organic conducting polymers is in the area of chemical and biological sensors. In many applications for sensors, the ability to detect low concentrations of specific analytes with high sensitivity and high selectivity is important. While high selectivity can be achieved by tuning or modifying the chemical and physical properties of CPNWs, high sensitivity can be obtained by operating them as field-effect transistors (FETs) because of the ability of FETs to amplify in-situ and to gate-modulate channel conductance. Additionally, the compatibility of FET-based sensors with well-developed microelectronic fabrication techniques makes miniaturization

feasible, enabling portability, small sample volumes, and high density arrays.

The pioneering studies of conducting polymer as the FET or switch devices and sensors were from Wrighton and colleagues, who demonstrated that the magnitude of the current between two microelectrodes connected by a thin film of conducting polymer depended upon the electrochemical potential of the conducting polymer (CP).^{3–5} They also demonstrated that the transistor action could also arise from conductivity modulation of the polymer due to the oxidation or reduction of the CPs as supported by ion incorporation from (or ion expulsion to) the electrolyte. Recently, there have been attempts to miniaturize the semiconducting CP materials to nanoscale dimensions. Tao and colleagues reported that in contrast to the smooth increase of conductance upon oxidation of polyaniline in bulk samples (gap of ~ 60 nm), the conductance switched discretely/abruptly between insulating (off) and conducting (on) states for the same polymer bridging a nanoscale gap (varying between 1 nm and a few tens of nanometers).⁶ In another report, electrochemical FET behavior of a mesh of polyaniline nanowires bridging two 10- μm -wide Pt electrodes separated by 2 μm and termed as conducting polymer nanowire electrode junctions (CPNEJs) was investigated.⁷ The objective of our study is to investigate the electronic properties of a true single CPNW-based transistor with fully insulated microelectrodes resulting in only the CPNW being exposed to the electrolyte to minimize any leakage currents that may arise due to the exposure of the microelectrodes to the electrolyte.

Materials and Methods

The electrodes were fabricated on a (100)-oriented silicon wafer with a chemical vapor deposition (CVD) grown, 1 μm thick insulator layer of low-stress Si_3N_4 film. A Cr adhesion layer and a ~ 3000 Å thick Au contact layer were then deposited,

* Corresponding authors. E-mail: myung@engr.ucr.edu. Tel.: (951) 827-7710. Fax: (951) 787-5696 (N.V.M.). E-mail: adani@engr.ucr.edu. Tel.: (951) 787-6419. Fax: (951) 787-5696 (A.M.).

[†] University of California, Riverside.

[‡] University of Pittsburgh.

[§] Present address: Chemistry Department, Missouri State University, Springfield, MO 65897.

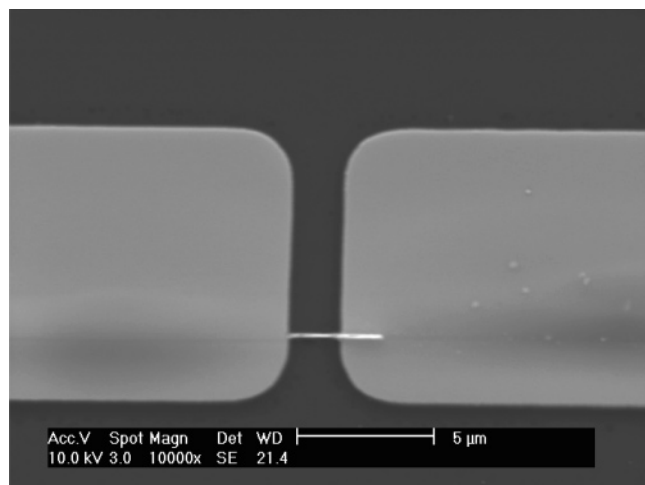


Figure 1. Scanning electron microscope image of a PANI nanowire.

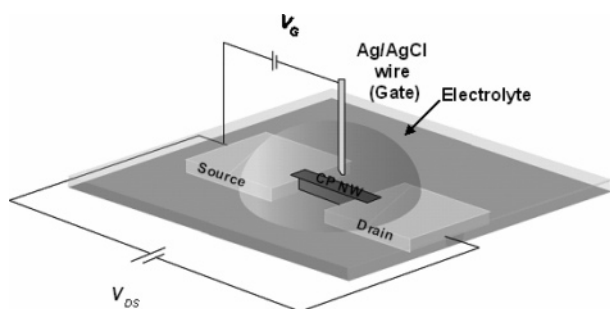


Figure 2. Schematic illustration of the single conducting polymer nanowire based electrolyte/liquid ion-gated FET device.

with contacts being patterned by lift-off. Thermally evaporated SiO₂ was then deposited on the wafer at room temperature followed by a coat of poly(methyl methacrylate) (PMMA) photoresist. Using e-beam lithographic patterning, the deposited SiO₂ and PMMA were selectively opened with reactive ion etching to form electrolyte channels. The widths and lengths of the electrolyte channels were fixed at 100 nm and 2.5 μm, respectively.

A three-electrode setup was used in a typical CPNW deposition experiment as was recently demonstrated by us.¹ Briefly, 2 μL of deoxygenated pyrrole (0.06 M in 0.01 M NaCl) or aniline (0.1 M in 0.1 M HCl) were placed in the electrolyte channel between the two electrodes, and the electropolymerization was performed in galvanostatic mode by applying a desired current while the potential of the working electrode was monitored continuously with respect to a Ag/AgCl wire pseudo-reference electrode. A Biologic Science VMP2 multi-channel potentiostat/galvanostat (Princeton Applied Research) was used for the electrochemical experiments. Typically, the potential increased from the open circuit potential to a value of ~2 V as the CPNW grew from the anode toward the cathode. When the CPNW made contact with the cathode, the potential dropped to almost zero. At this time, the process was terminated, the electrolyte solution was siphoned out, and the wafer was rinsed three times with deionized distilled water and dried. Figure 1 shows the scanning electron microscope image of a synthesized polyaniline (PANI) nanowire. The CPNWs were converted into FET devices by dispensing a fresh electrolyte solution onto the CPNWs and immersing a third electrode (Ag/AgCl wire) into the electrolyte medium. Figure 2 shows the schematic of the complete configuration in which the two gold electrodes served as the source and drain while the Ag/AgCl wire served as the electrolyte/liquid ion gate. The characteriza-

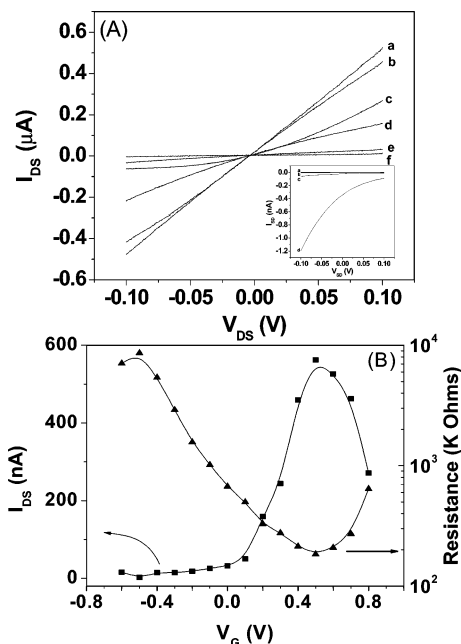


Figure 3. (A) Source-drain current (I_{DS}) vs source-drain voltage (V_{DS}) at different applied gate potentials (V_G values) for a PANI NW connecting two gold electrodes in pH 1 buffer. The sweep rate of V_{DS} = 50 mV/s. (a) V_G = 0.6 V, (b) V_G = 0.4 V, (c) V_G = 0.8 V, (d) V_G = 0.2 V, (e) V_G = 0.0 V, (f) V_G = -0.4 V. (inset) Source-drain current (I_{DS}) vs source-drain voltage (V_{DS}) at different applied gate potentials (V_G values) for a blank nanochannel connecting two gold electrodes in pH 1 buffer. The sweep rate of V_{DS} = 50 mV/s. (a) V_G = -0.8 V, (b) V_G = 0.4 V, (c) V_G = 0.6 V, (d) V_G = 0.8 V. (B) Plot of I_{DS} vs V_G (squares) and resistance vs V_G (triangles) at a V_{DS} of 0.1 V for a PANI NW.

tion of the electrolyte-gated FETs in buffered aqueous media was performed at ambient conditions. The ionic strengths of the buffer solutions were adjusted by NaCl solution to 0.1 M NaCl in order to normalize the background conductances. The gate potential (V_G) was set to different values while sweeping the source-drain voltage (V_{DS}) and monitoring the source-drain current (I_{DS}). A control device with a blank nanochannel between the two microelectrodes under identical measurement conditions exhibited minimal leakage currents of less than 3 orders of magnitude compared with the recorded CPNW I_{DS} values, confirming that the leakage currents were much less than the ones recorded for exposed electrodes⁷ due to complete insulation of our microelectrodes.

Results and Discussion

The electronic characteristics of single polyaniline (PANI) and polypyrrole (PPY) nanowires in FET mode were studied by monitoring I_{DS} while sweeping V_{DS} at different values of fixed V_G . As shown in Figure 3A, the resistance of the PANI nanowire (inverse of the slope of the I_{DS} - V_{DS} curve) was a function of the fixed V_G values. This dependence/relationship, best visualized from the plot of I_{DS} vs V_G (Figure 3B), showed that I_{DS} was negligible, i.e., the device was off at negative V_G values, as the PANI nanowire was in a reduced form and therefore insulating. Upon changing V_G to more positive values, a significant steady-state I_{DS} was observed, i.e., the device was turned on as the PANI NW was conducting. The threshold voltage (V_T), defined as the V_G at which the I_{DS} was effectively turned on, was between -0.3 and -0.2 V. This compares well with the V_T of -0.3 V reported for PANI nanowire electrode junctions.⁷ Increasing V_G to more positive potentials had the effect of oxidizing the nanowire resulting in a gradual increase

in I_{DS} to a maximum at ~ 0.5 V. Further increase of V_G resulted in a decrease of I_{DS} as the nanowire was fully oxidized. The resistance of the PANI nanowire connecting the two gold electrodes was calculated from the inverse of the slopes of the I_{DS} vs V_{DS} curves at any given V_G . As shown in Figure 3B, at V_G values that are less negative or more positive than V_T , the resistance of the PANI nanowire gradually decreased to a minimum at a V_G of ~ 0.5 V. Further increase of V_G to more positive values resulted in a gradual increase in the resistance of the nanowire due to overoxidation of the PANI as was previously observed for PANI films.⁵ Raman studies have indicated that degradation of polyaniline occurs after overoxidation at potentials greater than 0.8 V (vs standard calomel electrode (SCE)).⁸ The data clearly demonstrated that the resistance of the PANI nanowire depends on its gate potential with minimum resistance at a V_G of 0.5 V. This indicates that the PANI nanowire has a finite potential dependence window of high conductivity. It is also clearly evident (Figure 3B) that the resistance of the PANI nanowire can be modulated by almost 3 orders of magnitude by just varying the V_G . Similar device characteristics have been observed for PANI film-based triodes.^{3,5}

Transistor performance is usually judged by various parameters, including transconductance (g_m) and the on/off current ratio (I_{on}/I_{off}). Transconductance of the PANI nanowire FET was obtained from the slope of the linear region in the I_{DS} vs V_G plot (Figure 3B) at $V_{DS} = 0.1$ V. The maximum value of g_m for this particular PANI nanowire was about $2.2 \mu\text{S}$, which was over 2 orders of magnitude more than that reported for PANI film-based FETs⁹ and more than 4 orders of magnitude more than the values reported for FET based on camphorsulfonic acid doped electrospun polyaniline/polyethylene oxide nanofibers.¹⁰ In fact, normalizing the g_m to the PANI nanowire width of about ~ 100 nm gives a normalized transconductance of $22 \mu\text{S}/\mu\text{m}$ which is in the same range of $17\text{--}100 \mu\text{S}/\mu\text{m}$ reported for high performance SiNW-based FETs.¹¹

The ratio of I_{DS} at saturation (I_{on}) to I_{DS} at depletion (I_{off}) for FETs based on single PANI nanowires was approximately 230 for this PANI. This was comparable to the values previously reported for PANI nanowire electrode junction transistors when using Ag/AgCl as the gate electrode.⁷ However, it was over 2 orders of magnitude more than the I_{on}/I_{off} ratio reported for an FET based on camphorsulfonic acid doped electrospun polyaniline/polyethylene oxide nanofibers.¹⁰

Figure 4 shows the corresponding device characteristics of a single PPY nanowire FET. Like the PANI nanowire, the slopes of the I_{DS} – V_{DS} curves changed with variation in V_G (Figure 4A). It is evident that the V_T of this PPY nanowire was approximately -0.1 V when the device turns on and a significant steady-state value of I_{DS} was observed to reach a maximum at a V_G of 0.55 V (Figure 4B). The V_T compares well with -0.1 V observed for PPY nanowire electrode junction transistors.⁷ As evident in Figure 4B, at V_G values that are more positive than V_T , the resistance of the PPY nanowire decreases to a minimum (at about a V_G of 0.5 V). The maximum value of g_m for this PPY nanowire was about $1.3 \mu\text{S}$. Normalizing the g_m to the PPY width of ~ 100 nm gives a normalized transconductance of $13 \mu\text{S}/\mu\text{m}$ which is close to the normalized g_m values reported for high performance SiNW-based FETs.¹¹ On the other hand, the I_{on}/I_{off} ratio was 309 which was more than 3 times the value reported for PPY nanowire electrode junction transistors.⁷

Figure 5A and B show the effect of the variation of pH on the resistance vs V_G curves of PANI and PPY nanowires,

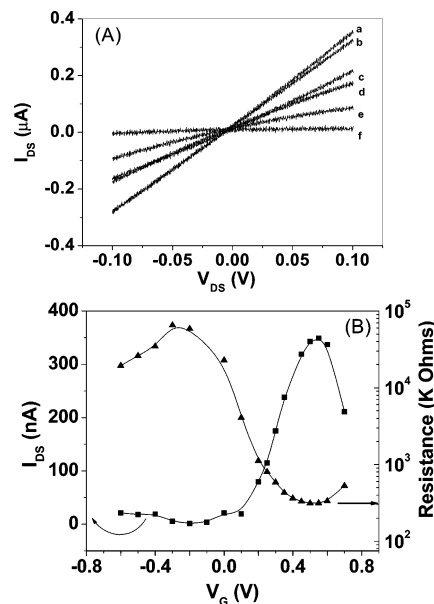


Figure 4. (A) Source-drain current (I_{DS}) vs source-drain voltage (V_{DS}) at different applied gate potentials (V_G values) for a PPY NW connecting two gold electrodes in pH 1 buffer. The sweep rate was fixed at 50 mV/s. (a) $V_G = 0.55$ V, (b) $V_G = 0.45$ V, (c) $V_G = 0.7$ V, (d) $V_G = 0.3$ V, (e) $V_G = 0.2$ V, (f) $V_G = 0.1$ V. (B) Plot of I_{DS} vs V_G (squares) and resistance vs V_G (triangles) at a V_{DS} of 0.1 V for a PPY NW.

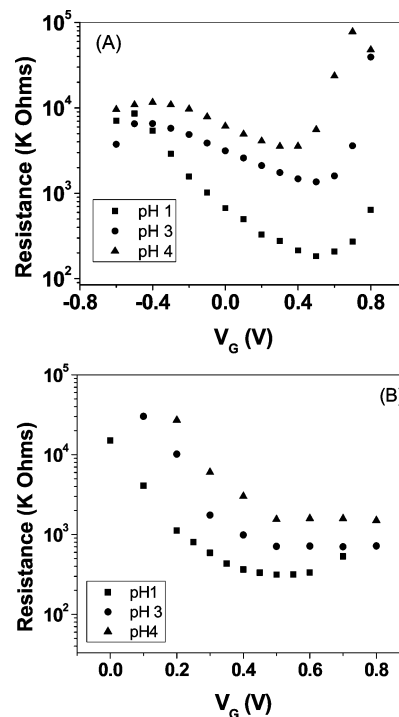


Figure 5. Plot of resistance of PANI (A) and PPY (B) NWs connecting two gold electrodes as a function of applied gate potential (V_G) in different pH solutions.

respectively. As expected, the resistances of nanowires increased with a pH increase, attributed to the lower conductivity of the polymers in less acidic or more basic media.^{12–14} The dependence of conductivity on pH is attributed to the protonation/deprotonation of the pyrrolic and the imine nitrogen in the PPY nanowire and PANI nanowire, respectively. Protonation results in the formation of delocalized radical cations and is accompanied by an increase in conductivity and a decrease in resistance.¹⁵ Thus, the conductivity of PANI nanowires and PPY nanowires does not only depend on the extent of oxidation but

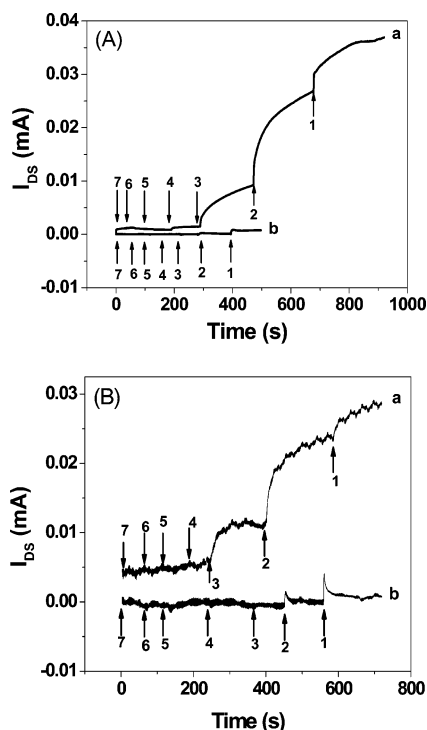


Figure 6. Dynamic responses of source-drain current (I_{DS}) flowing through PANI (A) and PPY (B) NWs in different pH solutions as a function of time at different gate potentials. For the PANI NW, V_G was fixed at 0.4 (a) and 0.8 V (b). For the PPY NW, V_G was fixed at 0.4 V (a) and 0.1 V (b). The source-drain voltage (V_{DS}) was 0.1 V in both cases. The arrows correspond to the points where the solution pHs were changed.

also on the extent of protonation of the polymers. Also, as expected, PANI NWs were much more sensitive to pH changes than PPY nanowires due to the possibility of more oxidation states in PANI because the imine nitrogen atoms in PANI can be protonated in whole or in part to give correspondingly different PANI salts.

Figure 6A presents the dynamic response of I_{DS} flowing through the FET-configured PANI nanowires when they were exposed to different pH solutions at gate potentials corresponding to more conducting ($V_G = 0.4$ V) and less conducting ($V_G = 0.8$ V) states for V_{DS} of 0.1 V. As shown (Figure 6A), the PANI nanowire was more sensitive to pH when the wire was more conducting ($V_G = 0.4$ V) in comparison to when it was less conducting ($V_G = 0.8$ V). Similar results were observed for PPY nanowires (Figure 6B), i.e. high pH sensitivity in more conducting states ($V_G = 0.4$ V) compared to less conducting states ($V_G = 0.1$ V). These results clearly demonstrated a simple yet powerful method of tailoring the sensitivity of the CPNW-based FET devices by modulating the gate potential.

Conclusions

We demonstrated the characteristics of FETs based on single conducting polymer nanowires. The CPNWs were deposited at ambient conditions using benign reagents within nanochannels between two gold electrodes in a manner that allowed the demonstration of transistor-like electronic devices through an

electrolyte-gated electrode approach. This is a major advantage over SiNW and CNT FET devices that require harsh synthetic conditions, post-synthesis functionalization, alignment, and positioning. Like other FET devices, the large change in electrical conductivity of CPNWs as a result of variation in the electrochemical potential formed the basis of the device function. The CPNW FET device can be turned on and off by electrical or chemical signals. This has major implications in chemical- and biosensing as this means that weak analytical signals which would have otherwise been undetectable could be readily detected. We also demonstrated that the CPNW FETs perform much better than CPNEJ FETs and CP film FETs in terms of g_m and I_{on}/I_{off} ratio values, and they perform very competitively when compared with the well-known SiNW FETs. Further, we demonstrated the rapid dynamic pH response of these CPNW FET devices and how the magnitude of the pH response can be amplified by the simple variation of V_G . These studies demonstrate the great potential that CPNWs have in 1-D-based FET technology as it is much easier to immobilize biomolecules in conducting polymers than in SiNWs and CNTs.¹⁶ Due to the obvious advantages of these CPNW FET devices, we are currently investigating the immobilization and multiplexed detection of pathogens and other biological molecules using these devices.

Acknowledgment. We acknowledge the support of this work by grants H94003-04-2-0404 from DOD/DARPA/DMEA, BES-0529330 from NSF, and GR-83237501 from the U.S. EPA. M.A.B. acknowledges the financial support from UC Graduate Research and Education in Adaptive Bio-Technology Training (GREAT) program.

References and Notes

- (1) Ramanathan, K.; Bangar, M. A.; Yun, M. H.; Chen, W. F.; Mulchandani, A.; Myung, N. V. *Nano Lett.* **2004**, *4* (7), 1237–1239.
- (2) Ramanathan, K.; Bangar, M. A.; Yun, M.; Chen, W.; Myung, N. V.; Mulchandani, A. *J. Am. Chem. Soc.* **2005**, *127* (2), 496–497.
- (3) Ofer, D.; Crooks, R. M.; Wrighton, M. S. *J. Am. Chem. Soc.* **1990**, *112* (22), 7869–7879.
- (4) McCoy, C. H.; Wrighton, M. S. *Chem. Mater.* **1993**, *5* (7), 914–916.
- (5) Paul, E. W.; Ricco, A. J.; Wrighton, M. S. *J. Phys. Chem.* **1985**, *89* (8), 1441–1447.
- (6) He, H. X.; Li, X. L.; Tao, N. J.; Nagahara, L. A.; Amlani, I.; Tsui, R. *Phys. Rev. B* **2003**, *68* (4).
- (7) Alam, M. M.; Wang, J.; Guo, Y. Y.; Lee, S. P.; Tseng, H. R. *J. Phys. Chem. B* **2005**, *109* (26), 12777–12784.
- (8) Sariciftci, N. S.; Kuzmany, H. *Synth. Met.* **1987**, *21* (2), 157–162.
- (9) Kuo, C. T.; Chiou, W. H. *Synth. Met.* **1997**, *88* (1), 23–30.
- (10) Pinto, N. J.; Johnson, A. T.; MacDiarmid, A. G.; Mueller, C. H.; Theofylaktos, N.; Robinson, D. C.; Miranda, F. A. *Appl. Phys. Lett.* **2003**, *83* (20), 4244–4246.
- (11) Cui, Y.; Zhong, Z. H.; Wang, D. L.; Wang, W. U.; Lieber, C. M. *Nano Lett.* **2003**, *3* (2), 149–152.
- (12) Chiang, J. C.; MacDiarmid, A. G. *Synth. Met.* **1986**, *13* (1–3), 193–205.
- (13) MacDiarmid, A. G.; Asturias, G. E.; Kershner, D. L.; Manohar, S. K.; Ray, A.; Scherr, E. M.; Sun, Y.; Tang, X.; Epstein, A. J. *Abstr. Pap. Am. Chem. Soc.* **1989**, *197*, 20-Poly.
- (14) MacDiarmid, A. G. *Angew. Chem., Int. Ed.* **2001**, *40* (14), 2581–2590.
- (15) Reghu, M.; Subramanyam, S. V. *Synth. Met.* **1991**, *41* (1–2), 455–458.
- (16) Wanekaya, A. K.; Chen, W.; Myung, N. V.; Mulchandani, A. *Electroanalysis* **2006**, *18* (6), 533–550.